Journal of Advanced Concrete Technology
Materials, Structures and Environment

Bearing stiffness of UHPC; an experimental investigation and a comparative study of regression and SVR-ABC models

Amin Khazaee, Mansour Ghalehnovi

Journal of Advanced Concrete Technology, volume 16 (2018), pp. 145-158

Related Papers Click to Download full PDF!

A Simplified Constitutive Model for Dowel Action across RC Cracks

Ali Reza Moradi, Masoud Soltani, Abbas Ali Tasnimi

Journal of Advanced Concrete Technology, volume10 (2012), pp. 264-277

Properties of ultra high performance concrete containing superfine cement and without silica fume

Rui Xiao, Zon-Cai Deng, Chenliang Shen

Journal of Advanced Concrete Technology, volume12 (2014), pp. 73-81

Influence of applied loads on the permeability behavior of ultra high performance concrete with steel fibers

Zhiming Ma, Tiejun Zhao, Xiaochuan Yao

Journal of Advanced Concrete Technology, volume14 (2016), pp. 770-781

Click to Submit your Papers

Japan Concrete Institute http://www.j-act.org

Scientific paper

Bearing Stiffness of UHPC; An Experimental Investigation and A Comparative Study of Regression and SVR-ABC Models

Amin Khazaee[1] and Mansour Ghalehnovi[2*]

Received 4 August 2017, accepted 20 March 2018 doi:10.3151/jact.16.145

Abstract

In this paper results of an experimental investigation on the bearing stiffness (K_f) of Ultra-High Performance Concrete (UHPC) under dowel bars are summarized. The effect of concrete strength, bar diameter, and location of the bar in concrete were investigated. By considering these parameters as input variables, several linear and nonlinear regressions and also Support Vector Regressions (SVRs) by incorporating different kernels are constructed, trained and tested to predict the K_f of UHPC. Comparing the results show that in the regression models, quadratic polynomial is more feasible in predicting the K_f of UHPC than other proposed functions and among the various kernels, SVR with radial basis function (RBF) kernel exhibits better results than other kernels.

1. Introduction

In a reinforced concrete member, especially in a beam, active mechanisms for shear transfer are as follows: 1.The force produced in shear bars that is significant after a diagonal crack, 2. Shear capacity of concrete in a part of the compression zone of the concrete that is not cracked, 3. The force from the aggregates interlock at both sides of the crack, 4. dowel action of flexural bars that compress the concrete in the lower part of crack and prevent from crack displacement through crack surface. Dowel action can be defined as follows: ability of longitudinal bars to transfer the force perpendicular to their axis. The distance between longitudinal axis of those parts on both sides of the crack that are not deformed is considered as dowel bar deformation (**Fig. 1-a**) (béton 1996). In **Fig. 1** (part b and c), examples of built-in interfaces and stress-induced interfaces are shown. Due to concrete crushing, the stress under the bars can be assumed to be roughly uniform close to critical sections at the ultimate condition (**Fig. 1-d**) (Dei Poli *et al*. 1992; Dulacska 1972; Soroushian *et al*. 1987).

In reinforced concrete cracks, aggregate interlock generally tolerates the shear force more. As loading continues and the crack width increases, the contribution of this mechanism decreases. Therefore, it is not effective in crack widths more than 1 mm (Maitra *et al*. 2009). Also in prefabricated connections and joints, aggregate interlock mechanism is not involved at all and has no contribution to shear transfer. In fact, in such connections, the only shear transfer factor is longitudinal bars (dowel mechanism).

In recent years, extensive experimental and analytical studies have been conducted on dowel mechanism. Maekawa and Qureshi (1997a) suggested a micro scale model for prediction of reinforcing bar behavior under the general condition of axial pullout and transverse displacement. The interaction of axial pullout and transverse dowel action was considered in formulation establishing. Also, Maekawa and Qureshi (1996) illustrated that interaction of pullout and transverse shear of steel at a crack is important and cannot be ignored. Then, Maekawa and Qureshi (1997b) presented a unified model to simulate the behavior of interface transfer mechanism. Soltani and Maekawa (2008) extended the model proposed by Maekawa and Qureshi (1997a) to path-dependent cyclic loading case.

Almost all presented models introduced Beam on Elastic Foundation (BEF) theory as the most suitable method for simulation of dowel bars behavior. Timoshenko and Lessels (1925) proposed BEF for simulating the behavior of dowel bars embedded in concrete. Then, they used BEF for analyzing force transfer mechanism in reinforced concrete pavements and cracked surfaces. According to BEF, longitudinal bar plays the role of the beam and its confining concrete plays the role of the elastic foundation. In this model, concrete foundation is simulated using elastic springs. If the bearing stiffness (K_f) is known, load-carrying capacity of longitudinal bars can be calculated easily (Moradi 2013).

During loading, K_f is the most important factor in dowel load-bearing. On the other hand, bearing stiffness is directly related to the concrete strength. Various researchers have presented different values for bearing stiffness in elastic state (Dei Poli *et al*. 1992; Finney 1956; Soltani and Maekawa 2008; Soroushian *et al*. 1987; Soroushian *et al*. 1986; Walraven and Reinhardt 1981). In linear state, bearing stiffness can be a constant number as in the traditional BEF models. However, in nonlinear behavior, K_f must be a function of the dis-

[1]Ph.D. Candidate, Ferdowsi University of Mashhad, Mashhad, Iran.
[2]Associate Professor, Ferdowsi University of Mashhad, Mashhad, Iran. *Corresponding author,
E-mail: ghalehnovi@um.ac.ir

placement or the shear value of dowel bar to model the damage due to the load increasing (Dei Poli *et al*. 1992; Moradi *et al*. 2012; Moradi *et al*. 2015). It should be mentioned that all previous K_f relationships were obtained by tests on normal strength concrete.

In recent years, prediction of mechanical properties of construction materials has attracted many researchers' attention. Using linear and nonlinear regression methods is one of the most popular techniques for predicting mechanical properties of concrete (Tsivilis and Parissakis 1995; Zain and Abd 2009). Many researches were conducted to predict different properties of concrete. Today, in addition to common regression techniques, machine learning approaches are widely used to predict the mechanical properties of the materials, concrete compressive strength (CCS), detection of diseases and so on. One of this machine learning approach which has been used in literature for prediction of CCS is Support Vector Regression (SVR) (Smola and Schölkopf, 2004). SVR is an extension of Support Vector Machines (SVMs), for solving nonlinear regression problems. The SVM which was first introduced by Vapnik (1999), is a powerful method in the category of statistical learning theory and its main application was in pattern recognition problems. Very promising results of SVM in various classification problems such as detecting construction materials in digital images (Rashidi *et al*. 2016), The electrocardiogram (ECG) beat classification (Zadeh and Khazaee 2011; Ebrahimzadeh *et al*. 2014; Khazaee and Ebrahimzadeh 2010), detection of Alzheimer's disease and mild cognitive impairment (Khazaee *et al*. 2015a; Khazaee *et al*. 2015b; Khazaee *et al*. 2016), and so on, made it a popular methodology. Interestingly, SVR also showed excellent performance in various prediction fields, such as failure prediction and reliability analysis (Behnia *et al*. 2016), backbreak prediction in blasting operation (Faradonbeh *et al*. 2016), and the likes. Recently, some authors used SVR to predict CCS (Gilan *et al*. 2012; Yuvaraj *et al*. 2013b; Chou and Tsai 2012; Yuvaraj *et al*. 2013a). However, despite the great potential of SVR models, they have not received the attention they deserve in the CCS prediction literature as compared to other research fields. In addition, it has been pointed out that the performance of SVR is greatly affected by the values of model parameters and yet there is no general rule to find appropriate SVR parameters (Cherkassky and Ma 2004). The popular methods of model parameter setting are grid search and gradient descent, which have drawbacks such as vulnerability to a local optimum. Evolutionary algorithms such as genetic algorithm (GA) and particle swarm intelligence (PSO) have been adopted to find a global optimum solution by proper setting of SVR model parameters. A new emergence global optimization algorithm is the artificial bee colony algorithm (ABC) (Karaboga and Akay 2009; Karaboga *et al*. 2014). ABC has been found to be a useful tool in many of the real world optimization problems, due to the simplicity, few numbers of control parameters, and outstanding performance (Karaboga *et al*. 2014). Some authors compared the performance of ABC with that of other optimization methods, such as the genetic algorithm, differential evolution, and PSO

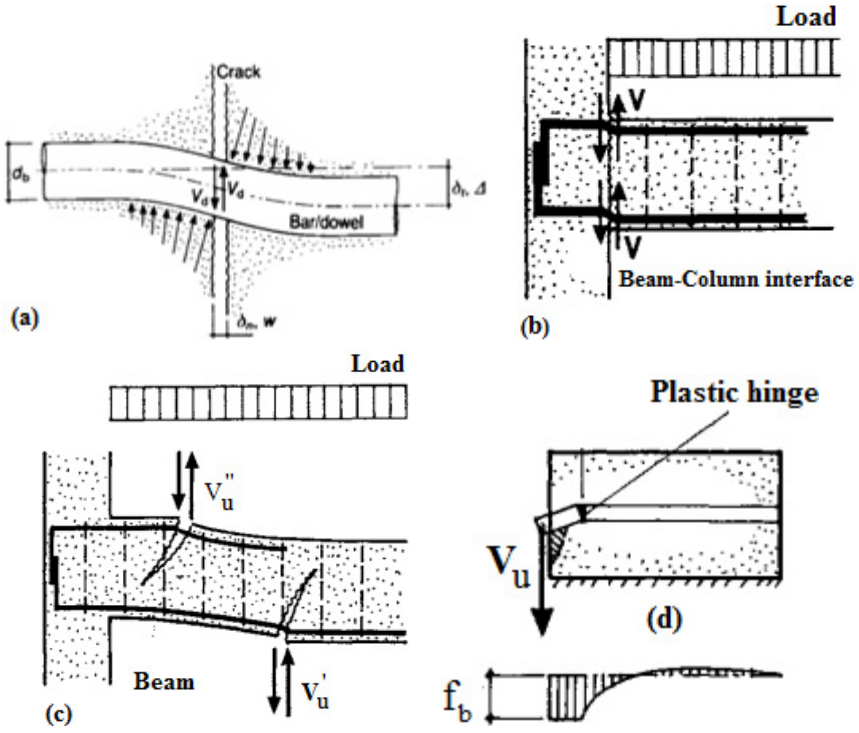

Fig. 1 Dowel action (a). Activation of dowel action due to relative displacement (béton 1996) (b). Built-in interfaces (c). Stress induced interfaces (d). Uniform stress distribution at ultimate condition (Dei Poli *et al*. 1992).

(Karaboga and Akay 2009; Kang *et al*. 2011). They showed that ABC is superior to the other methods in various problems such as signal processing, clustering, and geotechnical stability. Kang and Li (2015) used an intelligent response surface method for system probabilistic stability evaluation of soil slopes. They employed ABC to optimized SVR to establish the response surface to approximate the limit-state function.

Relations presented for bearing stiffness in the past are obtained by testing normal strength concrete specimens. In this study, 39 specimens of Ultra-High Performance Concrete (UHPC) are prepared and the K_f value of any sample is calculated by doing tests. Then, the bearing stiffness of ultra-high performance concrete samples are predicted using linear and nonlinear regression and SVR method.

2. Aim and methodology

One of the main parameters for determining dowel strength is bearing stiffness. Various researchers tried to determine K_f by doing different tests. Experimental researches conducted in the past were on normal strength concrete. The main aim of the present research is to achieve a suitable relation to predict the bearing stiffness of UHPCs. For this purpose, bearing stiffness is calculated for 39 specimens made up of UHPC and 9 different linear and nonlinear regressions functions are examined to predict K_f. The best function can be used for predicting K_f in UHPCs. Then the hybrid SVR-ABC (as a new method that proposed recently by researchers) with different kernels is used to evaluate ability of this algorithm in prediction of K_f , and the best kernel is introduced. Finally, a comparison between the best SVR kernel results with the best regression function is performed to evaluate that which one has worked more precisely. An overview of this study is shown in **Fig. 2**.

3. Modeling approach

3.1 Linear/nonlinear regression

Linear regression is a kind of regression analysis in which the relationship between one or more independent variables and a dependent variable is modeled using a linear equation. While in nonlinear regression, the aim is to find a suitable nonlinear equation to express the relationship between independent and dependent variables. The general form of regression models is as follows:

$$y = f(a_i + x_i) \tag{1}$$

In this relation, y, f, a_i and x_i are dependent variable, linear or nonlinear function, constants and independent variables, respectively. The main aim is to find the most suitable function f with the constants a_i. In the present research, 9 different linear and nonlinear functions are examined to predict K_f.

3.2 Support Vector Regression (SVR)

Support vector machine (SVM) is one of the most popular machine learning methods that has been widely applied to solve many learning tasks such as classification and regression (Vapnik 1999). Support vector regression (SVR) is a regression version of SVM which solves regression problems by use of an alternative loss function (Smola and Schölkopf 2004). In SVR, the original data x is mapped to a high dimensional feature space and then a linear regression problem is solved in this space. SVR formulation follows the principle of structural risk minimization instead of the principle of empirical risk minimization. In other words, SVR tries to minimize an upper bound of the generalization error instead of minimizing the prediction error on the training set. Consider a data set $\left[(x_i, y_i) \mid i = 1,...,l\right]$, where $\boldsymbol{x_i}$ is a D-dimensional input vector, y_i is a scalar output or target, and l is the number of points. The nonlinear relationship between the input and the output can be described by a regression function as:

$$f(x) = w^T \varphi(x) + b \tag{2}$$

where $f(x)$ = forecasting values; $\varphi(x)$ = nonlinear mapping function; and w and b = coefficients to be adjusted.

The coefficients w and b are estimated by minimizing the regularized risk function

$$R(C) = \mathrm{R}_{emp} + \frac{1}{2}\|w\|^2 = C\frac{1}{l}\sum_{i=1}^{l} L_\varepsilon\left[y_i, f(x_i)\right] + \frac{1}{2}\|w\|^2 \tag{3}$$

$$L_\varepsilon(y_i, f(x_i)) = \begin{cases} |y_i - f(x_i)| - \varepsilon & |y_i - f(x_i)| \geq \varepsilon \\ 0 & |y_i - f(x_i)| < \varepsilon \end{cases} \tag{4}$$

Where R(C) and R_{emp} = regression and empirical risks. In Eq. (3), the first item is the empirical error, which is estimated by the ε-insensitive loss function in Eq. (4). The second item is the regularization. The value C is the trade-off parameter between the first and second terms of the equation. The parameter ε can be viewed as a tube

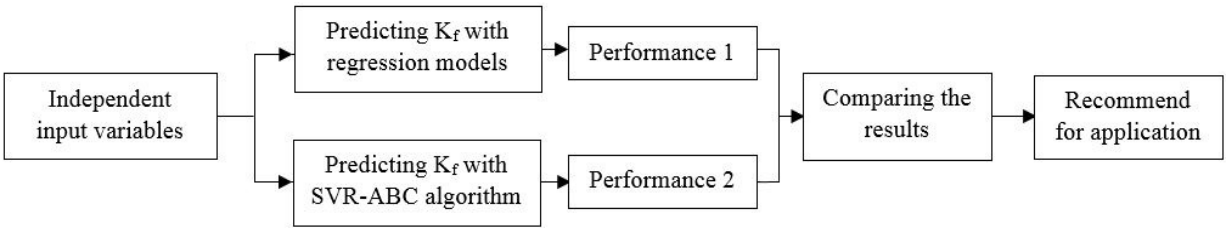

Fig. 2 Overview of the research.

size equivalent to the approximation accuracy of the training data.

Two positive slack variables ξ and ξ^* are introduced to represent the distance from the actual values to the corresponding boundary values of the ε-tube. Then minimization of Eq. (3) is converted into the following constrained form:

$$\text{Minimize } R(w,\xi,\xi^*) = \frac{1}{2}\|w\|^2 + C\sum_{i=1}^{l}(\xi_i + \xi_i^*) \tag{5}$$

$$\text{Subject to } \begin{cases} y_i - w\varphi(x_i) - b \le \varepsilon + \xi_i \\ w\varphi(x_i) + b - y_i \le \varepsilon + \xi \\ \xi_i, \xi_i^* \ge 0 \end{cases} \tag{6}$$

This optimization formulation can be transformed into the dual problem by introducing Lagrange multipliers as:

$$\begin{aligned} \text{Minimize } R(\alpha_i,\alpha_i^*) = &-\frac{1}{2}\sum_{i,j=1}^{l}(\alpha_i+\alpha_i^*)(\alpha_j+\alpha_j^*)K(x_i,x_j) \\ &-\varepsilon\sum_{i=1}^{l}(\alpha_i-\alpha_i^*) + \sum_{i=1}^{l} y_i(\alpha_i+\alpha_i^*) \end{aligned} \tag{7}$$

$$\text{Subject to } \sum_{i=1}^{l}(\alpha_i+\alpha_i^*) = 0,\ 0 \le \alpha_i,\ \alpha_i^* \le C \tag{8}$$

where $\alpha_i + \alpha_i^*$ = Lagrange multipliers and $K(x_i,x_j) = \varphi(x_i)^T\varphi(x_j)$ =kernel function.

The most applicable kernel function is the radial basis function (RBF) kernel:

$$K(x_i,x_j) = \exp\left(-\gamma\|x_i - x_j\|^2\right) \tag{9}$$

where γ = kernel parameter.

The RBF kernel has only one parameter to be determined, and SVR with a RBF kernel exhibits excellent nonlinear forecasting performance (Su *et al*. 2014, 2013).

The coefficient of Equation (2) can be obtained by the Lagrange multipliers as:

$$w = \sum_{i=1}^{l}(\alpha_i+\alpha_i^*)\varphi(x_i) \tag{10}$$

The regression function of SVR can be expressed as:

$$f(x) = \sum_{i=1}^{l}(\alpha_i+\alpha_i^*)K(x_i,x) + b \tag{11}$$

Based on Karush-Kuhn-Tucker's conditions for solving quadratic programming problems, only some of $(\alpha_i - \alpha_i^*)$ in Eq. (11) are held as nonzero values. The corresponding data points of $(\alpha_i - \alpha_i^*) \ne 0$ are support vectors, which are employed in determining the decision function. There are three user-determined parameters, *C, γ*, and *ε,* the selection of which plays an important role in SVR performance.

3.2.1 Artificial Bee Colony (ABC)

Artificial bee colony (ABC) algorithm is one of the most recently introduced algorithms, inspired by the intelligent behavior of honey bees (Karaboga *et al*. 2014). It is a simple algorithm like particle swarm optimization (PSO) and does not have many parameters like genetic algorithms (GA). Its parameters are only common parameters like colony size and maximum cycle number. ABC provides a population-based search in which a colony of artificial forager bees search for artificial food sources with high nectar amount. To apply ABC, the considered optimization problem is first converted to the problem of finding the best parameter vector which minimizes an objective function. Three essential components of ABC algorithm includes: employed and unemployed foraging bees, and food sources. The first two components, employed and unemployed foraging bees, search for rich food sources, which is the third component, close to their hive. Employed bees are associated with specific food sources. Unemployed bees include onlooker and scout bees. Onlookers choose a food source by watching the dance of employed bees within the hive. Scouts search for food sources randomly.

In ABC, position of food sources represents possible solution of the problem while the amount of nectar of food source represents the quality or fitness of that solution. Employed and onlooker bees fly around in a multi-dimensional search space and choose food sources depending on the experience of themselves and their nest mates, and adjust their positions. Scout bees fly and choose the food sources randomly without using experience. If the nectar amount of a new source is higher than that of the previous one in their memory, they memorize the new position and forget the previous one. Thus, ABC system combines local search methods, carried out by employed and onlooker bees, with global search methods, managed by onlookers and scouts, attempting to balance exploration and exploitation process. The ABC algorithm can be split into four different phases, namely: initialization phase, employed bees phase, onlooker bees phase and scout bees phase. At the initialization phase a population of NS solutions is initialized randomly and control parameters are set. The value of NS=NP/2, number of food sources, is equal to the number of employed bees and NP is the population size. Each solution u_i (i=1, 2… NS) holds *n* variables u_{ij} (j=1, 2, …, n) which are to be optimized so as to minimize the objective function. The artificial bees (employed bees, onlooker bees and scout bees) thus perform a cyclic search until a maximum cycle number according to some specific rules. At the employed bees phase, each employed bees search for new candidate food source position (v_i) on the neighborhood of the previously selected food source (u_i) to update feasible solutions. The quality (fitness) of the candidate solution is compared to the old one. If the fitness of the new solution is equal to or higher than the previous solution, the old one is re-

placed by the candidate one (greedy selection). A neighbor solution can be determined from the old one using the following formula:

$$v_{ij} = u_{ij} + \phi_{ij}(u_{ij} - u_{kj}) \tag{12}$$

Where k and j are randomly chosen indexes in range [1 NS] and [1 n], respectively ($k \neq i$) and ϕ_{ij} is a uniformly distributed random number within the range of [−1,1].

In the onlooker bees' phase, employed bees share the information on the food sources they have found with the onlooker bees returning to their hive. Then each onlooker bee probabilistically selects one food source depending on this information. The probability value p_i of a food source with, which is chosen by an onlooker bee can be calculated as:

$$p_i = \frac{fit_i}{\sum_{j=1}^{NS} fit_j} \tag{13}$$

where fit_i is the fitness value of food source I and is calculated from the objective function of food source as (in minimization problems):

$$fit_i = \begin{cases} \dfrac{1}{1+f_i} & f_i \geq 0 \\ 1+\left|f_i\right| & f_i < 0 \end{cases} \tag{14}$$

By increasing the fitness value of a food source the probability of selection increases. After a food source u_i is selected by an onlooker bee, a new food source V_i in the neighborhood of selected onlooker bee is determined. The new food source can be calculated by using Eq. (12). Then its fitness value is computed and solutions u_i and v_i are compared by a greedy selection. Therefore, more onlooker bees are recruited to richer food sources and consequently positive feedback behavior appears. If the position of an employed bees cannot be improved further through a limited number of cycles, in the scout bees phase, then that solution are abandoned and becomes a scout bee. Scouts are unemployed bees that choose their food sources randomly. The maximum abandonment limit is specified by the user. A new food source is determined by the scout bees for abandoned source as follows:

$$u_{ij} = u_{jmin} + rand \times (u_{jmax} - u_{jmin}) \tag{15}$$

where u_{jmin} and u_{jmax} are lower and upper bounds of u_{ij}, respectively, and $rand$ is a random number between 0 and 1 drawn from a uniform distribution. The flowchart of ABC algorithm is shown in **Fig. 3**.

4. Modeling performance criterions

The MAPE (Mean Absolute Percent Error) measures the size of the error in percentage terms. It is calculated as the average of the unsigned percentage error, as shown in the below:

$$\text{MAPE} = \frac{1}{n}\sum_{i=1}^{n}\left|\frac{y-\bar{y}}{y}\right| \times 100 \tag{16}$$

where y is the actual value, $\bar{y}$ is the predicted value and n is the total number of values.

Root mean squared error (RMSE) is a frequently used measure of the differences between values predicted by a model and the values actually observed, and is calculated by the following equation:

$$RMSE = \sqrt{\frac{\sum (y_j - \bar{y}_j)^2}{n}} \tag{17}$$

R squared, is a number that indicates the proportion of the variance in the dependent variable that is predictable from the independent variable

$$R^2 = 1 - \left(\frac{\sum_j (y_j - \bar{y}_j)^2}{\sum_j \left(y_j - \frac{\sum y_j}{n} \right)^2} \right) \tag{18}$$

5. Properties of materials, mixing process and sample preparation

5. 1 Properties of materials

Materials of ultra-high performance concrete include Portland cement, silica fume, quartz powder, silica sand, super-plasticizer and water. One of the most important materials in the mixture of ultra-high performance concrete is quartz powder. The mean diameter of its particles is 0.01 mm. Quartz powder is a hard material that improves the properties of matrix in the concrete. Size of silica sand particles used ranges from 0.15 to 0.8 mm. Some of the advantages of silica sand include high hardness and widely available. Cement Type II is used for preparing the specimens.

5.2 Mixing process

All the dry constituents are mixed together until they are homogeneously mixed. Then, part of water and half of the super-plasticizer were added to the mixture and the mixing process continued until the materials were mixed completely. Then, the remaining water and super-plasticizer were added. The mix design of the concrete is obtained from Rahdar and Ghalehnovi (2016) and is given in **Table 1**.

5.3 Sample preparation

The purpose of the test is to calculate the bearing stiffness under longitudinal bars. Specimens were cast from ultra-high performance concrete, a ribbed bar was embedded to half its diameter on the top surface and designed as dowel bars bearing against the concrete core

Table 1 Mix design of the consumed concrete per cubic meter(Rahdar and Ghalehnovi 2016).

	Portland cement type II (kg)	Silica fume (kg)	Quartz powder (kg)	Silica sand (kg)	Super-plasticizer (kg)	Water (lit)
Mix design 1	670	200	285	1020	16.75	178
Mix design 2	670	200	215	1000	30	154

as shown in **Fig. 4**. For specimen design, sample model presented by Soroushian *et al*. (1987) is used. The only difference is that ultra-high performance concrete is used in these tests. Longitudinal bars were partially embedded into the concrete (**Fig. 4.a**). Thirty nine samples were tested to study the effect of different parameters on the bearing stiffness. The parameters include: 1. Bar diameter, 2. Concrete strength 3. Concrete block width (side cover of bar), 4. Concrete block depth. It should be mentioned that actual stress distribution in concrete is not uniform under longitudinal bars along it. However, Due to concrete crushing (**Fig. 1-d**), the stress under the bars can be assumed to be roughly uniform close to critical sections at the ultimate condition (such as near the beam-column interface in prefabricated structures (**Fig. 1-b**)).

After removing the samples from the mold, they were cured in water for 28 days. The cylindrical compressive strengths of the samples f_c during the test are presented in **Table 2** together with other properties.

The value of K_f is strongly related to the quality of the concrete immediately under the bar. So, even when the same concrete composition is used, a scatter is obtained, depending on the position of the bar during cast-

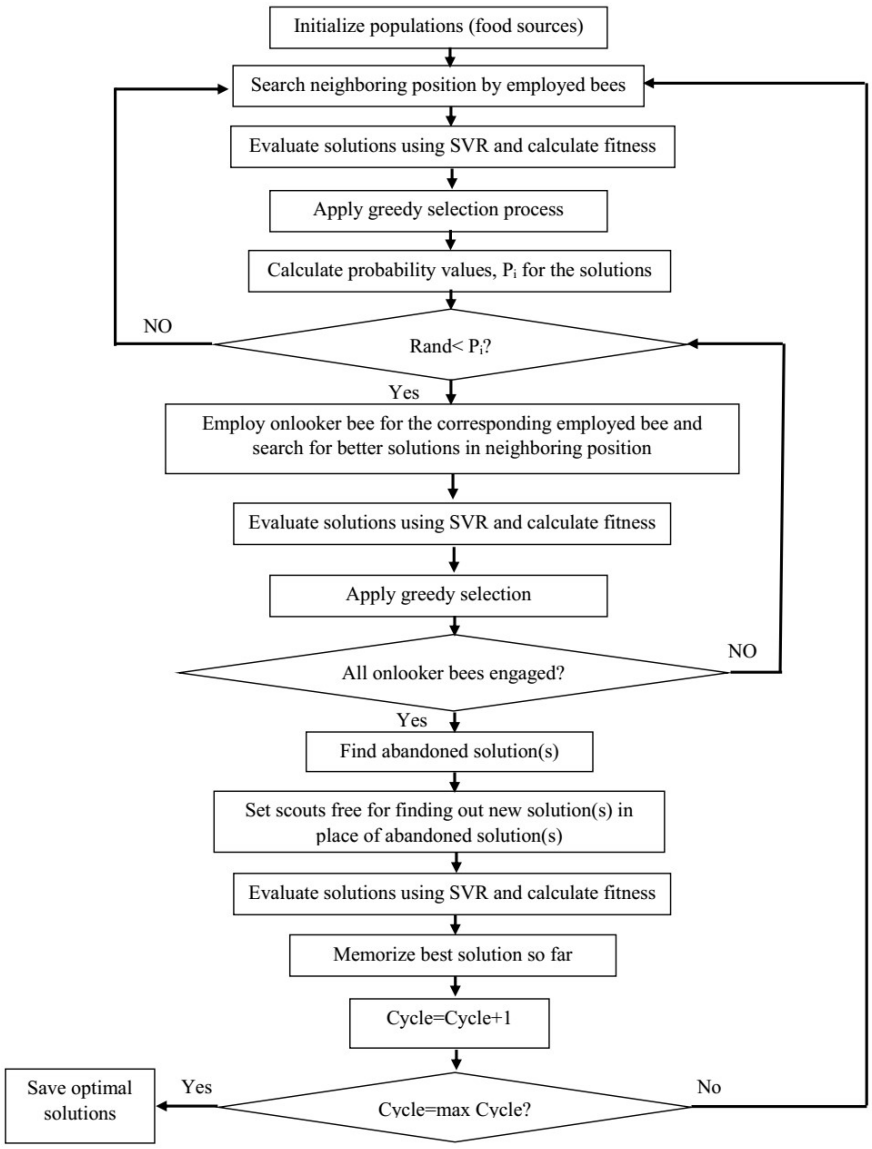

Fig. 3 The whole procedure of the SVR-ABC method.

Table 2 Properties of the test specimens and the test results.

Code	Series	b(mm)	d(mm)	l(mm)	w(mm)	d_b(mm)	f_c(MPa)	K_f(MPa/mm)	Failure mode*
S1	I	150	230	150	75	25	96.7	106.74	SYM
S2		150	230	150	75	25	106.8	129.65	SYM
S3		150	230	150	75	25	105.5	95.91	SYM
S4		150	230	150	75	25	105.5	167.96	SYM
S5	II Bar diameter	150	230	150	75	32	105.3	185.3	SYM
S6		150	230	150	75	32	105.3	131.6	SYM
S7		150	230	150	75	32	91.5	114.93	ASYM
S8		150	230	150	75	20	101	282.3	SYM
S9		150	230	150	75	20	101	249.16	SYM
S10		150	230	150	75	20	91.5	199.42	SYM
S11		150	230	150	75	12	108.1	344.95	SYM
S12		150	230	150	75	12	108.1	371.3	ASYM
S13		150	230	150	75	12	91.5	294.65	SYM
S14	III Concrete strength	150	230	150	75	25	95.9	119.08	ASYM
S15		150	230	150	75	25	95.9	136.35	ASYM
S16		150	230	150	75	25	103.3	168.57	SYM
S17		150	230	150	75	25	103.3	236.07	SYM
S18		150	230	150	75	25	106.7	145.55	SYM
S19		150	230	150	75	25	106.7	139.41	SYM
S20		150	230	150	75	25	108.9	164.4	SYM
S21		150	230	150	75	25	108.9	116.23	SYM
S22		150	230	150	75	25	108.9	135.68	SYM
S23		150	230	150	75	25	73.5	110.4	SYM
S24		150	230	150	75	25	70.4	100.34	SYM
S25		150	230	150	75	25	75.4	98.4	SYM
S26	IV Block width	75	230	150	37.5	25	110.4	71.21	SYM
S27		75	230	150	37.5	25	108.1	55.74	SYM
S28		75	230	150	37.5	25	91.6	91.5	SYM
S29		75	230	150	37.5	25	91.6	101.34	SYM
S30		230	230	150	115	25	110.4	195.11	SYM
S31		230	230	150	115	25	109.6	182.07	SYM
S32		230	230	150	115	25	91.6	154.87	SYM
S33		230	230	150	115	25	91.6	150.48	SYM
S34	V Block depth	150	150	150	75	25	111.3	131.45	SYM
S35		150	150	150	75	25	105.5	118.29	SYM
S36		150	150	150	75	25	105.5	144.93	SYM
S37		150	300	150	75	25	106.7	145.44	SYM
S38		150	300	150	75	25	101.6	95.56	SYM
S39		150	300	150	75	25	101.6	114.72	SYM

***** Symmetrical failure**: SYM,** Asymmetrical failure**: ASYM.**

ing. When the direction of the bar is parallel to the direction of casting a greater value of K_f can be expected than in the case of a bar perpendicular to this direction, since during the vibration a local segregation of water under the bar can be expected, resulting in a lower concrete quality. So, in sample preparing, the direction of casting was placed parallel to the direction of casting.

5.4 Test method

The test set-up and sample loading are shown in **Fig. 5**. Loading was static and force control in all tests. The force is distributed uniformly by a rigid steel plate along the bar. The displacement of dowel bar under load is measured by two electric LVDTs with high precision and values are recorded against the applied load. It is worthy to note that the concrete sample is on a rigid beam during loading.

6. Experimental test results

The stress-displacement curve was plotted for all samples. The samples' behavior was elastic until failure. Failure of samples occurred suddenly and was accompanied by crack development under the bar into the concrete sample. In most cases, the crack splits the concrete block into two almost symmetrical parts (**Fig. 6a**). Of course, asymmetrical failure occurred in a few samples (**Fig. 6b**). To calculate the bearing stiffness, the load applied to the sample is divided by the effective cross-sectional area of the bar ($f_b = P / [l \times d_b]$) and then, its curve is plotted against displacement. Afterwards, a line is fitted to the points of the curve and its slope is considered as the bearing stiffness. For brevity, one curve from each series is selected and shown in **Fig. 7**. In this figure, the curves S11, S14, S28 and S34 represents series II (rebar diameter), III (concrete

strength), IV (block width) and V (block depth) respectively. The bearing stiffness of the test samples range from 55.74 MPa/mm to 371.30 MPa/mm. K_f values of different samples are presented in the last column of **Table 2**.

7. Results and discussion

7.1 Empirical test results

The results in **Table 2** are obtained according to the tests performed on the concrete samples with no transverse bars. Test samples have different dimensions and compressive strengths (70-111 MPa) and are affected by

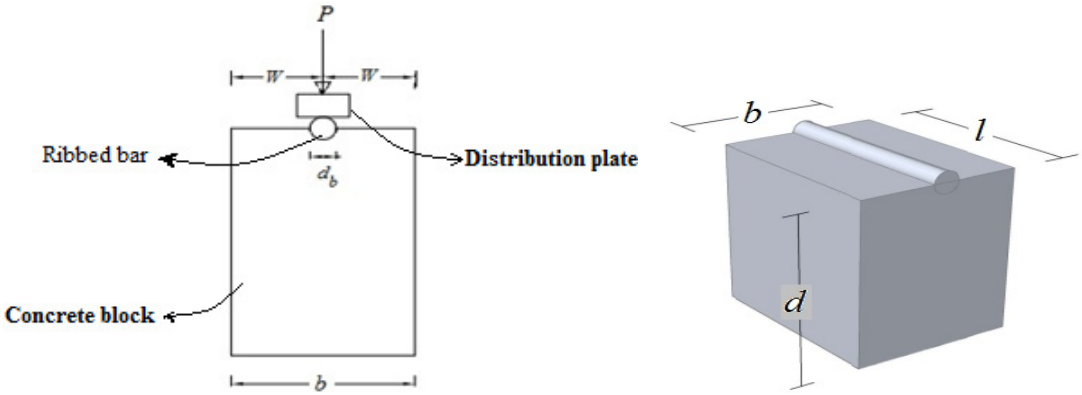

(a) (b)

Fig. 4 Dimensional and loading details: (a) overall dimensions of test specimen with partially embedded ribbed bar, and (b) sample loading using force distribution plate.

Fig. 5 General view of test set-up.

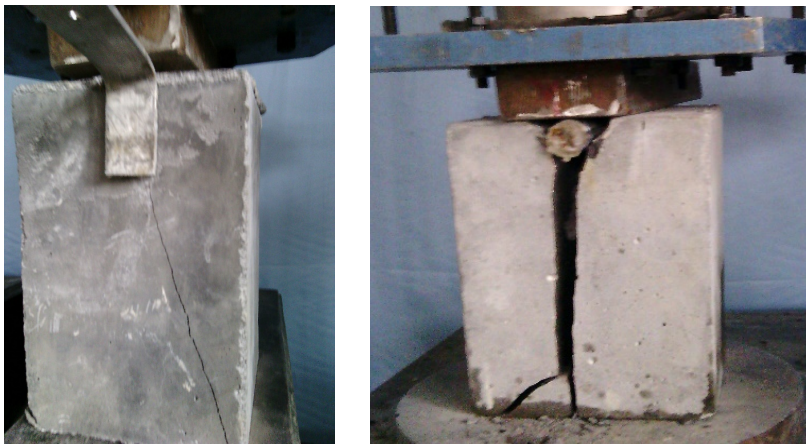

(a) (b)

Fig. 6 Failure of samples. (a) Symmetrical failure (occurred in most samples), (b) Asymmetrical failure.

Table 3 Data division to training set and testing set.

Training set	S1, S4, S5, S7, S8, S10, S12, S13, S15, S17, S19, S21, S22, S23, S25, S27, S29, S31,S32, S35, S36, S37, S38
Testing set	S2, S3, S6, S9, S11, S14, S16, S18, S20, S24, S26, S28, S30, S33, S34, S39

a longitudinal bar with different dimensions. The results of the experimental test show that the bearing stiffness increases as the longitudinal bar diameter decreases and the concrete strength increases. In addition, the increase in the side cover of the longitudinal bar results in the increase in the bearing stiffness. However, the bearing stiffness was not sensitive to variations in specimen depth. In this study, sample model presented by (Soroushian *et al*. 1987) is used, but since the concrete materials are changed and due to the high compressive strength of the test samples, the previous empirical relations are not accurate enough to predict K_f of UHPC and new relations must be introduced. The precision of Soroushian empirical relation for K_f, which is obtained by testing on normal strength concrete, is compared in **Table 8** with the results of the best models in this research.

7.2 Linear/nonlinear regression

Generally, two classes of functions are used to perform the regression. In the first class, bar diameter d_b and concrete compressive strength f_c are used as the independent input variables, because in previous empirical relations (Dei Poli *et al*. 1992; Soltani and Maekawa 2008; Soroushian *et al*. 1987), two parameters of d_b and f_c are used to determine the bearing stiffness. In the second class, the equations 6 to 9, the parameters including concrete block depth (d) and the side cover of the bar (w) are also introduced as independent variables in addition to the parameters d_b and f_c. Functions used for regression include first and second degree polynomial functions, fractional functions, polynomial fractional and power fractional functions. To train the proposed models and test them, the test results are classified into two groups including 23 training sets and 16 testing sets (**Table 3**). In **Table 4**, characteristics of the functions used for regression are presented. Functions are analyzed by Minitab Software. To calculate the constants, Levenberg-Marquardt algorithm is used. The evaluated coefficients of the proposed models are presented in **Table 5**. It should be mentioned that the constants are obtained based on the results of 23 samples of the training set. To test the proposed relations, the results of the remaining 16 samples are used (**Table 3**). MAPE, RMSE and R^2 are measured based on the Eqs. (16), (17) and (18), respectively and are presented in **Table 6**. To examine the precision of the proposed relations better, the results of the proposed models and those from the experiment are compared in the curves in **Fig. 8**. In this curve, the horizontal axis shows the samples' numbers and the vertical axis shows the bearing stiffness values.

The results of **Table 6** and also **Fig. 8** show that among the two-variable models, model-2 with the second order polynomial function has the best response, while in this group model-1 with the first order polynomial function has the least accuracy in determining the responses. Among models with four input variables, model-7 with the second order polynomial function has the best response, whereas in this group model-6 with the first order polynomial function has the least precision in determining the responses. In other words, according to the results, it can be concluded that the rela-

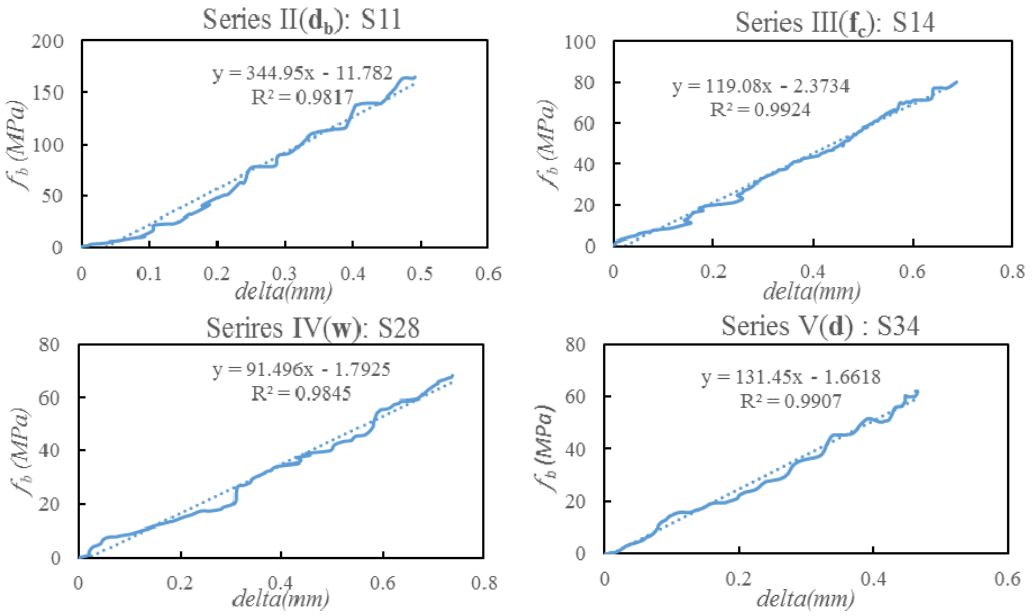

Fig. 7 Bearing stress versus displacement of the bar (the slope of the curve shows the bearing stiffness).

Table 4 Proposed Linear/nonlinear regression models to predict K_f.

Independent Variables	Model	Linear/nonlinear regression model*
f_c , d_b	Model1	$a_0 + a_1 f_c + a_2 d_b$
	Model2	$a_0 + a_1 f_c + a_2 d_b + a_3 f_c^2 + a_4 d_b^2$
	Model3	$a_0 + a_1 (f_c / d_b)$
	Model4	$a_0 + a_1 (f_c / d_b) + a_2 (f_c / d_b)^2$
	Model5	$a_0 (f_c^{a_1} / d_b^{a_2})$
f_c , d_b , w , d	Model6	$a_0 + a_1 w + a_2 d_b + a_3 f_c + a_4 d$
	Model7	$a_0 + a_1 w + a_2 d_b + a_3 f_c + a_4 d + a_5 w^2 + a_6 d_b^2 + a_7 f_c^2 + a_8 d^2$
	Model8	$a_0 + a_1 (f_c / d_b) + a_2 (w / d_b) + a_3 (d / d_b)$
	Model9	$a_0 + a_1 (f_c / d_b)^{a_2} + a_3 (w / d_b)^{a_4} + a_5 (d / d_b)^{a_6}$

* f_c: concrete compressive strength, d_b: bar diameter, w: side cover of the bar, d: block depth

Table 5 Evaluated coefficients of regression models.

Model	a_0	a_1	a_2	a_3	a_4	a_5	a_6	a_7	a_8
Model-1	78.102	0.840	1.000	-	-	-	-	-	-
Model-2	312.297	1.304	-11.696	-	-	-	-	-	-
Model-3	356.775	7.228	-43.628	-0.032	0.753	-	-	-	-
Model-4	-28.262	43.344		-	-	-	-	-	-
Model-5	31.631	20.142	1.981	-	-	-	-	-	-
Model-6	239.753	1.125	-11.708	1.268	-0.036	-	-	-	-
Model-7	-483.888	4.620	-36.368	11.813	2.938	-0.023	0.596	-0.054	-0.007
Model-8	-36.157	28.714	27.331	-1.844	-	-	-	-	-
Model-9	-865.177	3.449	2.050	864.199	0.088	02.5E-12	10.546	-	-

Table 6 Evaluation of regression models for training and testing tries.

Model	Training			Test			Variables
	R^2	MAPE%	RMSE	R^2	MAPE%	RMSE	
Model-1	0.554	30.071	48.545	0.586	29.439	40.377	f_c,d_b
Model-2	0.686	23.610	40.734	0.706	23.788	34.418	
Model-3	0.645	26.411	43.329	0.642	26.402	37.642	
Model-4	0.649	25.289	43.041	0.648	25.661	37.676	
Model-5	0.633	27.426	44.052	0.654	27.141	38.583	
Model-6	0.617	25.769	44.999	0.740	23.140	33.458	w, f_c,d_b,d
Model-7	0.796	18.583	32.826	0.843	15.907	25.936	
Model-8	0.713	21.231	38.978	0.812	18.505	28.426	
Model-9	0.734	21.064	37.499	0.816	18.969	28.101	

tionship between bearing stiffness and input variables cannot be a linear relationship, since the models with first order polynomial function has the least accuracy in both groups. The Model-7 has the maximum R^2 and the minimum MAPE and RMSE among all proposed models. The curves in the **Fig. 8** show that the results of Model-7 are more consistent with the empirical results compared to other models. To analyze the Model-7 more, the curve in the **Fig. 9** was plotted. In this figure, which is hereafter called as X–Y plot, the horizontal axis shows the predicted K_f values based on the Model-7 and the vertical axis shows the results of empirical test. In an X-Y curve, the closer the points to the diagonal line, the better prediction could be judged for the model. As it can be observed in this figure, the proposed model has low precision for determining the answer in some cases. It is due to the low number of data for extracting the nonlinear function coefficient.

7.3 SVR-ABC

In **Fig. 3**, ABC algorithm flowchart is presented. Also, the structure of the input–output of the modeler systems is schematically shown in **Fig. 10**. In this figure, the input parameters are (i) concrete compressive strength (f_c), (ii) bar diameter (d_b), (iii) side cover of the bar (w) and (iv) block depth (d), and K_f is the output parameter.

Since in linear and nonlinear regressions, functions with four independent variables gave better answers, SVR-ABC algorithm is trained only with four input variables in this section.

23 samples are used for training and 16 samples are used for testing as in **Table 3**. In **Table 7**, R^2, MAPE and RMSE values are presented for different kernels. In addition to this table, the curve in **Fig. 11** shows that the

Table 7 Evaluation of SVR kernels for training and testing tries.

Model	Training			Testing			Input variables
	R^2	MAPE%	RMSE	R^2	MAPE%	RMSE	
rbf kernel	0.803	9.362	32.238	0.888	15.925	24.435	w,f_c,d_b,d
sigmoid kernel	0.569	21.934	47.743	0.750	20.110	32.791	
poly1 kernel	0.585	22.126	46.838	0.770	18.633	31.437	
poly2 kernel	0.662	20.111	42.256	0.807	18.049	28.838	
poly3 kernel	0.296	22.529	61.008	0.438	19.744	49.151	

results of RBF kernel are more consistent with K_f values from the experiment. For this reason, K_f values from RBF kernel are plotted in X-Y curve (**Fig. 12**) to compare them better with the empirical results.

As it is evident from the **Fig. 12**, the predicted values of some samples in the training set are significantly different from those values of empirical results. It is due to the low number of data for training SVR model. Since the total number of data used for training is low, a few numbers of unacceptable predicted values resulted in worse R^2 and RMSE values for the training set than the testing set. Moreover, division of the data into training and testing sets becomes very important and sometimes the movement of some data among these groups highly affects the level of error in any group.

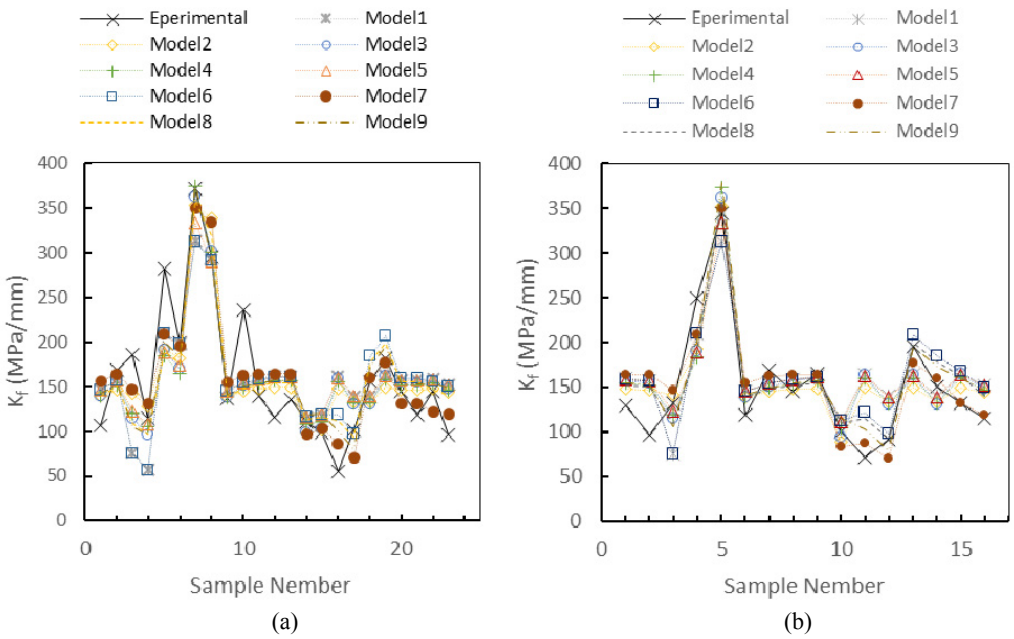

Fig. 8 Comparison of regression models with experimental results: (a) training set and (b) testing set.

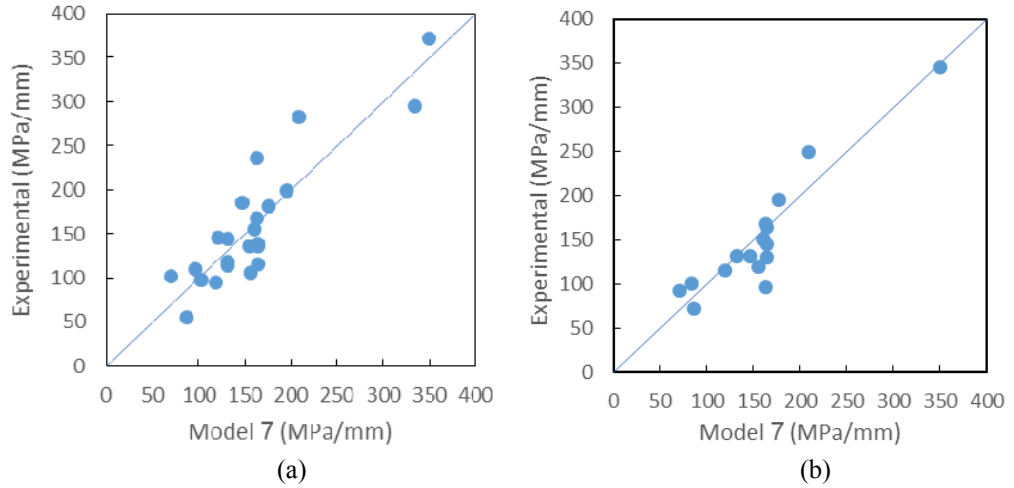

Fig. 9 Model-7 predictions vs. experimental results of K_f: (a) training set and (b) testing set.

Table 8 Comparing of Model7 and RBF kernel for testing records.

Model	Training			Testing		
	R^2	MAPE%	RMSE	R^2	MAPE%	RMSE
rbf kernel	0.803	9.362	32.238	0.888	15.925	24.435
Model7	0.796	18.583	32.826	0.843	15.907	25.936
Soroushian et al., 1987*	0.478	29.303	52.492	0.503	45.536	28.401

* $K_f = 127 \frac{f_c^{0.5}}{d_b^{\frac{2}{3}}}$

7.4 Comparison of regression with SVR

The results of the best regression function (Model-7) and the best kernel in SVR models (RBF kernel) are compared with the test results of K_f in **Table 8**. For more comparison, the results of Soroushian empirical relation for K_f are compared in **Table 8** with the results of this test. According to this table, it can be concluded

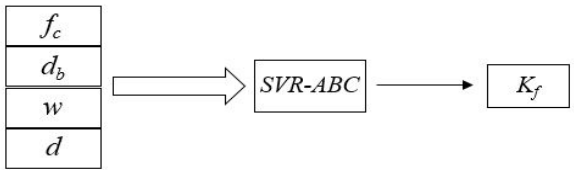

Fig. 10 Schematic structure of modeler system.

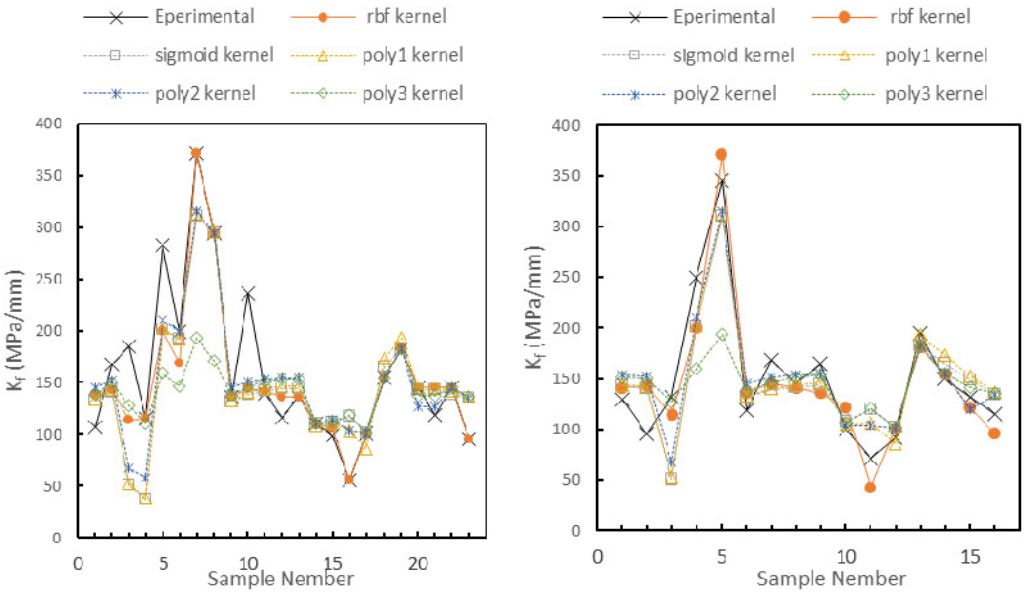

Fig. 11 Comparison of SVR kernels with experimental results: (a) training set, and (b) testing set.

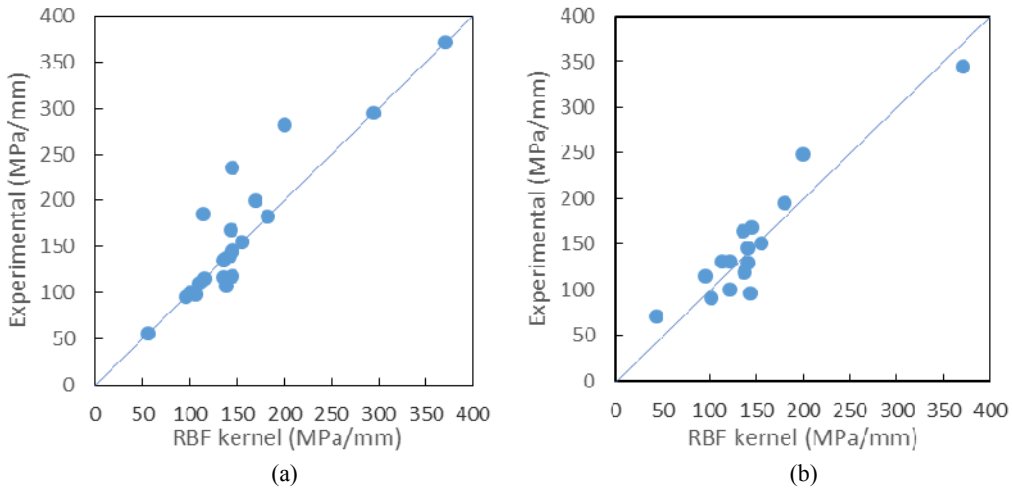

Fig. 12 RBF kernel predictions vs. experimental results of K_f: (a) training set,and (b) testing set.

that Soroushian's empirical relation for K_f based on normal strength concrete, has not enough precision for predicting K_f in ultra-high performance concretes.

According to **Table 8**, RBF kernel almost in all cases provided better answers than the nonlinear regression model, i.e. Model-7. The reason for this finding might be of the insufficient amount of data required for developing a regression model, while the SVR-ABC algorithm could recognize the relationships with lower data for their distributed and parallel computing nature.

In the hybrid SVR-ABC approach an ABC employed to optimize SVR model. Only a few studies use ABC for finding the best regression model (Kang and Li 2015; Khazaee and Khazaee 2017). ABC is a recently proposed optimization method that has many advantages compared to the other evolutionary algorithms. It has a strong global search optimum ability and, at the same time, is fast, easy to implement and few parameters to tune compared to the other optimization algorithms such as genetic algorithms and ant colony. Thus, the proposed SVR-ABC approach is faster than the other approaches while it is easy to implement as mentioned by Khazaee and Khazaee (2017).

8. Conclusions

In this paper results of an experimental investigation on the bearing stiffness (K_f) of Ultra-High Performance Concrete (UHPC) under dowel bars are summarized. The empirical results show that as the longitudinal bar diameter decreases and the concrete strength increases, the bearing stiffness increases. In addition, the increase in the side cover (block width) of the longitudinal bar results in an increase in the bearing stiffness. However, the increase in the sample depth does not affect it.

Since previous empirical equations for calculating bearing stiffness are obtained by testing on normal strength concrete, in this paper different empirical relations are presented to predict the bearing stiffness by performing linear and nonlinear regressions on the empirical results of UHPC. Among the relations presented, second degree polynomial function with four input variables, Model-7, gave better results than other proposed models.

To examine the capability of machine learning method, the results were examined using SVR-ABC algorithm. Among all kernels employed, RBF kernel gave much better results. Comparing the results from the Model-7 and SVR with RBF kernel, it is observed that SVR with RBF kernel answers have lower errors in K_f prediction than Model-7.

References

Behnia, A., Ranjbar, N., Chai, H. K. and Masaeli, M., (2016). "Failure prediction and reliability analysis of ferrocement composite structures by incorporating machine learning into acoustic emission monitoring technique." *Construction and Building Materials,* 122**,** 823-832.

Béton, C. E.-I. D. (1996). *RC elements under cyclic loading: state of the art report*, Thomas Telford.

Cherkassky, V. and Ma, Y. (2004. CPractical selection of SVM parameters and noise estimation for SVM regression." *Neural networks,* 17**,** 113-126.

Chou, J.-S. and Tsai, C.-F., (2012). "Concrete compressive strength analysis using a combined classification and regression technique." *Automation in Construction,* 24**,** 52-60.

DeI Poli, S., Di Prisco, M. and Gambarova, P. (1992). "Shear response, deformations, and subgrade stiffness of a dowel bar embedded in concrete. *Structural Journal,* 89**,** 665-675.

Dulacska, H., (1972). "Dowel action of reinforcement crossing cracks in concrete." *Journal Proceedings*, 754-757.

Ebrahimzadeh, A., Shakiba, B. and Khazaee, A., (2014). "Detection of electrocardiogram signals using an efficient method." *Applied Soft Computing,* 22**,** 108-117.

Faradonbeh, R. S., Monjezi, M. and Armaghani, D. J., (2016). "Genetic programing and non-linear multiple regression techniques to predict backbreak in blasting operation." *Engineering with Computers,* 32**,** 123-133.

Finney, E., (1956). "Structural design considerations for pavement joints." *Journal of the American Concrete Institute,* 28**,** 1-28.

Gilan, S. S., Jovein, H. B. and Ramezanianpour, A. A., (2012). "Hybrid support vector regression–Particle swarm optimization for prediction of compressive strength and RCPT of concretes containing metakaolin." *Construction and Building Materials,* 34**,** 321-329.

Kang, F. and Li, J., (2015). "Artificial bee colony algorithm optimized support vector regression for system reliability analysis of slopes." *Journal of Computing in Civil Engineering,* 30**,** 04015040.

Kang, F., Li, J. and Ma, Z., (2011). "Rosenbrock artificial bee colony algorithm for accurate global optimization of numerical functions." *Information Sciences,* 181**,** 3508-3531.

Karaboga, D. and Akay, B., (2009). "A comparative study of artificial bee colony algorithm." *Applied mathematics and computation,* 214**,** 108-132.

Karaboga, D., Gorkemli, B., Ozturk, C. and Karaboga, N., (2014). "A comprehensive survey: artificial bee colony (ABC) algorithm and applications." *Artificial Intelligence Review,* 42**,** 21-57.

Khazaee, A. and Ebrahimzadeh, A., (2010). "Classification of electrocardiogram signals with support vector machines and genetic algorithms using power spectral features." *Biomedical Signal Processing and Control,* 5**,** 252-263.

Khazaee, A., Ebrahimzadeh, A. and Babajani-Feremi, A., (2015a). "Application of advanced machine learning methods on resting-state fMRI network for identification of mild cognitive impairment and

Alzheimer's disease." *Brain Imaging and Behavior*, 1-19.

Khazaee, A., Ebrahimzadeh, A. and Babajani-feremi, A., (2015b). "Identifying patients with Alzheimer's disease using resting-state fMRI and graph theory." *Clinical Neurophysiology,* 126, 2132-2141.

Khazaee, A., Ebrahimzadeh, A. and Babajani-Feremi, A., (2016). "Application of advanced machine learning methods on resting-state fMRI network for identification of mild cognitive impairment and Alzheimer's disease." *Brain imaging and behavior,* 10, 799-817.

Khazaee, A. and Khazaee, A., (2017). "Compressive strength prediction of high performance concrete using artificial bee colony algorithm." *Revista Romana de Materiale-Romanian Journal of Materials,* 47, 387-395.

Maekawa, K. and Qureshi, J., (1996). "Embedded bar behavior in concrete under combined axial pullout and transverse displacement." *Doboku Gakkai Ronbunshu,* 1996, 183-195.

Maekawa, K. and Qureshi, J., (1997a). "Computational model for reinforcing bar embedded in concrete under combined axial pullout and transverse displacement." *Concrete Library of JSCE,* 29, 217-233.

Maekawa, K. and Qureshi, J., (1997b). "Stress transfer across interfaces in reinforced concrete due to aggregate interlock and dowel action." *Doboku Gakkai Ronbunshu,* 1997, 159-172.

Maitra, S. R., Reddy, K. and Ramachandra, L., (2009). "Load transfer characteristics of dowel bar system in jointed concrete pavement." *Journal of Transportation Engineering,* 135, 813-821.

Moradi, A., (2013). "*A universal constitutive model for simulate stress transfer across RC cracks and interfaces under cyclic multiaxial deformations.*" Thesis, (Ph.D). Tarbiat Modares University: Tehran.

Moradi, A. R., Soltani, M. and Tasnimi, A. A., (2012). "A simplified constitutive model for dowel action across RC cracks." *Journal of Advanced Concrete Technology,* 10, 264-277.

Moradi, A. R., Soltani, M. and Tasnimi, A. A., (2015). "Stress-transfer behavior of reinforced concrete cracks and interfaces." *ACI Structural Journal,* 112, 69-80.

Rahdar, H. and Ghalehnovi, M., (2016). "Post-cracking behavior of UHPC on the concrete members reinforced by steel rebar." *Computers and Concrete,* 18, 139-154.

Rashidi, A., Sigari, M. H., Maghiar, M. and Citrin, D., (2016). "An analogy between various machine-learning techniques for detecting construction materials in digital images." *KSCE Journal of Civil Engineering,* 20, 1178-1188.

Smola, A. J. and schölkopf, B., (2004). "A tutorial on support vector regression." *Statistics and computing,* 14, 199-222.

Soltani, M. and Maekawa, K., (2008). "Path-dependent mechanical model for deformed reinforcing bars at RC interface under coupled cyclic shear and pullout tension." *Engineering Structures,* 30, 1079-1091.

Soroushian, P., Obaseki, K. and Rojas, M. C., (1987). "Bearing strength and stiffness of concrete under reinforcing bars." *ACI Materials Journal,* 84(3), 179-184.

Soroushian, P., Obaseki, K., Rojas, M. C. and Sim, J., (1986). "Analysis of dowel bars acting against concrete core." *Journal Proceedings*, 83(4), 642-649.

Su, J., Wang, X., Liang, Y. and Chen, B., (2013). "GA-based support vector machine model for the prediction of monthly reservoir storage." *Journal of Hydrologic Engineering,* 19, 1430-1437.

Su, J., Wang, X., Liang, Y. and Chen, B., (2014). "GA-based support vector machine model for the prediction of monthly reservoir storage." *Journal of Hydrologic Engineering,* 19, 1430-1437.

Timoshenko, S. and Lessels, J., (1925). "*Applied elasticity. westinghouse technology*." Night School Press, East Pittsburgh, Pennsylvania.

Tsivilis, S. and Parissakis, G., (1995). "A mathematical model for the prediction of cement strength." *Cement and concrete research,* 25, 9-14.

Vapnik, V. N., (1999). "An overview of statistical learning theory." *IEEE transactions on neural networks,* 10, 988-999.

Walraven, J. and Reinhardt, H., (1981). "Concrete mechanics. Part A: Theory and experiments on the mechanical behavior of cracks in plain and reinforced concrete subjected to shear loading." *NASA STI/Recon Technical Report N,* 82.

Yuvaraj, P., Murthy, A. R., Iyer, N. R., Sekar, S. and Samui, P., (2013a). "Support vector regression based models to predict fracture characteristics of high strength and ultra high strength concrete beams." *Engineering Fracture Mechanics,* 98, 29-43.

Yuvaraj, P., Ramachandra Murthy, A., Iyer, N. R., Sekar, S. K. and Samui, P., (2013b). "Support vector regression based models to predict fracture characteristics of high strength and ultra high strength concrete beams." *Engineering Fracture Mechanics,* 98, 29-43.

Zadeh, A. E. and Khazaee, A., (2011). "High efficient system for automatic classification of the electrocardiogram beats." *Annals of biomedical engineering,* 39, 996-1011.

Zain, M. F. M. and Abd, S. M., (2009). "Multiple regression model for compressive strength prediction of high performance concrete." *Journal of applied sciences,* 9, 155-160.